


Fast, multiplane line-scan confocal microscopy using axially distributed slits: supplement

JEAN-MARC TSANG,^{1,*}  HOWARD J. GRITTON,^{1,2} SHOSHANA L. DAS,^{1,3} TIMOTHY D. WEBER,¹  CHRISTOPHER S. CHEN,^{1,3} XUE HAN,^{1,4} AND JEROME MERTZ^{1,4} 

¹*Department of Biomedical Engineering, Boston University, 44 Cummington Mall, Boston, MA 02215, USA*

²*Department of Comparative Biosciences, University of Illinois at Urbana-Champaign, Urbana, IL 61802, USA*

³*Wyss Institute for Biologically Inspired Engineering, Harvard University, Boston, MA 02115, USA*

⁴*Photonics Center, Boston University, 8 Saint Mary's Street, Boston, MA 02215, USA*

*jmtsang@bu.edu

This supplement published with The Optical Society on 9 February 2021 by The Authors under the terms of the [Creative Commons Attribution 4.0 License](#) in the format provided by the authors and unedited. Further distribution of this work must maintain attribution to the author(s) and the published article's title, journal citation, and DOI.

Supplement DOI: <https://doi.org/10.6084/m9.figshare.13664855>

Parent Article DOI: <https://doi.org/10.1364/BOE.417286>

Fast, multiplane line-scan confocal microscopy using axially distributed slits: supplemental document

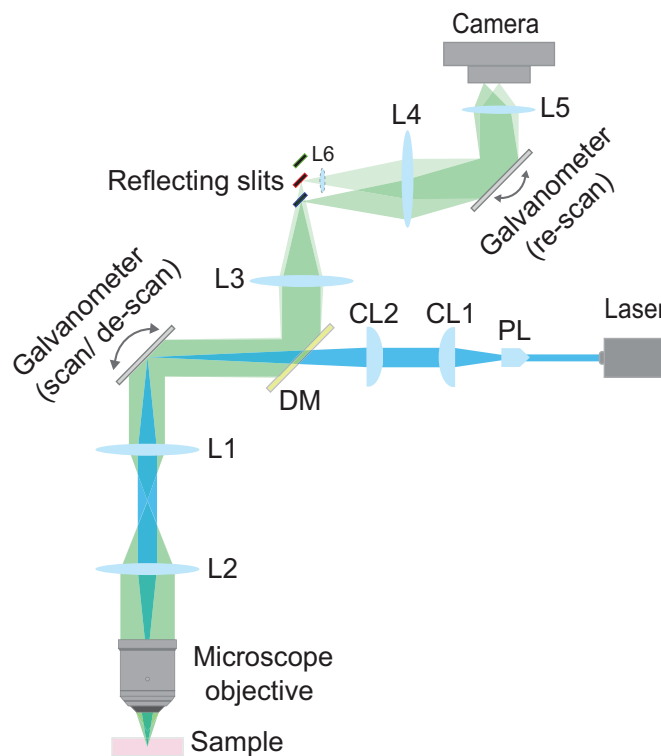


Fig. S1. Schematic of line-scan multi-z confocal microscope with labeled optical components (see Table S1).

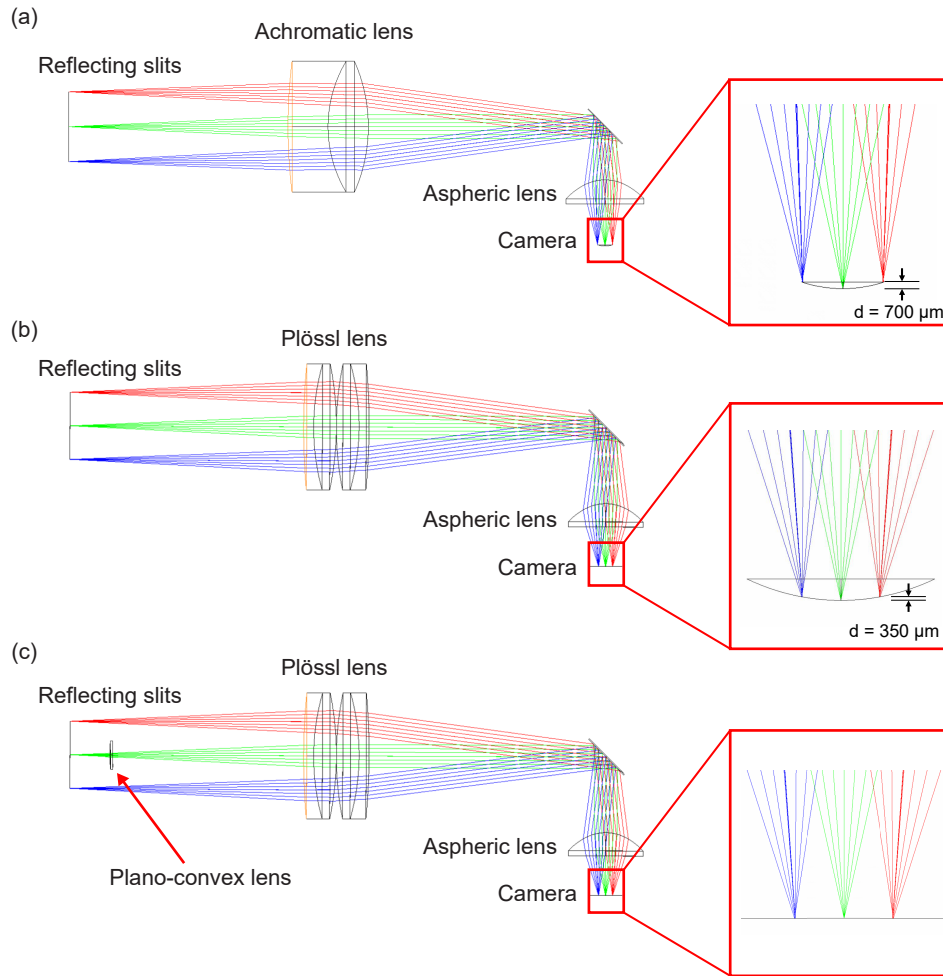


Fig. S2. (a) Ray diagram of the original detection unit. Inset shows the field curvature at the camera sensor. (b) Ray diagram of the detection unit using a Plössl scan lens inferred to have an effective focal length of 156 mm. Inset shows the field curvature is still $350 \mu\text{m}$ across the camera sensor. (c) Ray diagram of the detection unit using both a Plössl scan lens and a correction lens inserted just after the middle slit. Inset shows that the three slits are now properly focused on the camera.

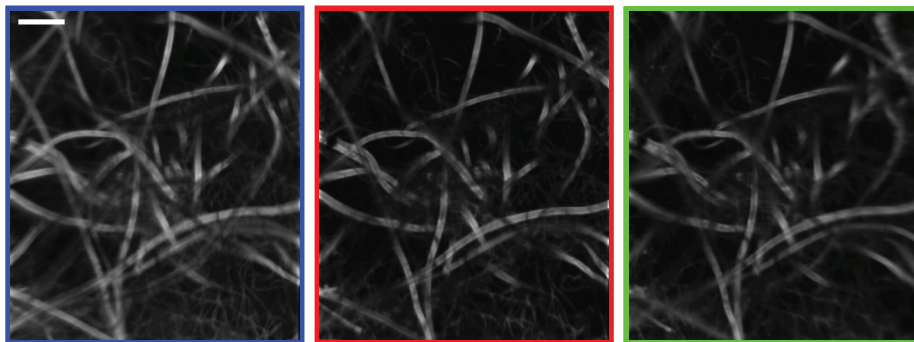


Fig. S3. Images of *Aspergillus conidiophores*, after applying elastic transforms, where a same sample plane is separately recorded by the three detection channels. As expected, the images acquired by the deepest and shallowest channels have lower resolution at the edges due to aberrations and residual astigmatism from off-axis imaging. Scale bar, $100 \mu\text{m}$.

Table S1. Description of the optical components used.

Component	Description	Part Number, Vendor
PL	Powell lens, 10° fan angle, 1.2 mm beam width, $\varnothing = 8.9$ mm	LOCP-8.9R10-1.2, Laserline Optics
CL1	Plano-convex cylindrical lens, $f = 50$ mm, $\varnothing = 1$ in	LJ1695RM-A, Thorlabs
CL2	Plano-convex cylindrical lens, $f = 75$ mm, $\varnothing = 1$ in	LJ1703RM-A, Thorlabs
DM	Quad band dichroic	ZT405/488/561/640 rpc, Chroma
L1	Achromatic doublet, $f = 150$ mm, $\varnothing = 2$ in	AC508-150-A-ML, Thorlabs
L2	Achromatic doublet, $f = 200$ mm, $\varnothing = 2$ in	ACT508-200-A-ML, Thorlabs
L3	Achromatic doublet, $f = 150$ mm, $\varnothing = 2$ in	AC508-150-A-ML, Thorlabs
L4	2 \times Achromatic doublet, $f = 300$ mm, $\varnothing = 75$ mm	88-594-INK, Edmund Optics
L5	Aspheric lens, $f = 32$ mm, $\varnothing = 45$ mm	AHL45-32-P-U-780, Asphericon
L6	Plano-convex lens, $f = 500$ mm, $\varnothing = 1$ in	LA1908-A, Thorlabs

Table S2. Characterization of the resolution spatial homogeneity for the Olympus 20 \times objective. The lateral FWHMs of the point spread functions (PSF) are measured at the center (0) and two extrema (+/-) of the excitation lines at each axial plane (deep, center, shallow), before and after applying the elastic transforms.

PSF Location (along line)	Before transform			After transform		
	Deep (μm)	Center (μm)	Shallow (μm)	Deep (μm)	Center (μm)	Shallow (μm)
+	5.1	4.1	5.4	5.3	4.1	5.9
0	5.3	4.2	5.3	5.5	4.2	5.6
-	5.3	4.3	5.4	5.7	4.3	5.8

Table S3. Characterization of the resolution spatial homogeneity for the Optem 20 \times objective. The lateral FWHMs of the point spread functions (PSF) are measured at the center (0) and two extrema (+/-) of the excitation lines at each axial plane (deep, center, shallow), before and after applying the elastic transforms.

PSF Location (along line)	Before transform			After transform		
	Deep (μm)	Center (μm)	Shallow (μm)	Deep (μm)	Center (μm)	Shallow (μm)
+	5.4	4.2	5.5	5.5	4.2	5.7
0	5.4	4.3	5.4	5.4	4.3	5.5
-	5.4	4.4	5.5	5.4	4.4	5.7